Chemistry of Metals and Alloys

Chem. Met. Alloys 13 (2020) 14-22
Ivan Franko National University of Lviv
www.chemetal-journal.org

Reciprocal $K_2TeI_6 + Rb_2TeBr_6 \leftrightarrow K_2TeBr_6 + Rb_2TeI_6$ system: phase relations, crystal and electronic structures

I. BARCHIY[1]*, O. ZUBAKA[1], E. PERESH[1], V. SIDEY[1], O. KOKHAN[1], I. STERCHO[1], A. FEDORCHUK[2,3], M. PIASECKI[4]

[1] *Department of Chemistry, Uzhgorod National University, Pidgirna St. 46, 88000 Uzhgorod, Ukraine*
[2] *Department of Inorganic and Organic Chemistry, Lviv National University of Veterinary Medicine and Biotechnologies, Pekarska St. 50, 79010 Lviv, Ukraine*
[3] *Department of Physical Chemistry of Fossil Fuels, Institute of Physical-Organic Chemistry and Coal Chemistry named after L.M. Lytvynenko, National Academy of Sciences of Ukraine, Naukova St. 3a, 79060 Lviv, Ukraine*
[4] *Institute of Chemistry, Environment Protection and Biotechnology, Jan Dlugosz University, Armii Krajowej St. 13/15, 42200 Częstochowa, Poland*
* *Corresponding author. E-mail: igor.barchiy@uzhnu.edu.ua*

Received May 25, 2020; accepted July 3, 2020; available on-line November 1, 2020
https://doi.org/10.30970/cma13.0400

The stability of the $K_2TeBr_6(I_6)$ and $Rb_2TeBr_6(I_6)$ compounds with perovskite structures was assessed within the idealized model of hard spheres (Goldschmidt's rule). The possibility of formation of solid solutions along sections of the reciprocal system $K_2TeI_6 + Rb_2TeBr_6 \leftrightarrow K_2TeBr_6 + Rb_2TeI_6$ was considered according to the quantitative criteria of Vozdvyzhensky. The K_2TeBr_6–Rb_2TeI_6 system was investigated by DTA and X-ray diffraction and the phase diagram was constructed. The binary system is of the invariant eutectic type and characterized by the formation of limited solid solutions. On the basis of crystallographic data the bonds lengths in the crystal structures were compared with the covalent and ionic radii of the atoms. The results showed that the chemical bonds in the $K_2TeBr_6(I_6)$ and $Rb_2TeBr_6(I_6)$ ternary compounds are of the mixed (combined) type – iono-covalent with a larger ionic component. The electronic structures of the $K_2(Rb_2)TeBr_6(I_6)$ compounds were calculated by the *ab initio* quantum-mechanical DFT method.

Halide perovskite / Phase diagram / Crystal structure / *Ab initio* calculations / Electronic structure

Introduction

The obtaining of new materials with luminescent, optical and other properties is an important task of inorganic materials science. Complex halides cause sustained interest among inorganic materials that are promising for use in modern semiconductor devices, such as solar cells. Metal-organic halide perovskites have high photoelectric performance [1-3]. The power conversion efficiencies of solar cells based on perovskites reach over 20% and approach by their parameters silicon-based photovoltaics [4-8]. However, their commercial use is limited by two drawbacks: the organic cation reduces the stability of the perovskite structure, and the lead content worsens the toxicity. To increase the stability of the structure, isovalent substitution of the organic cation by an alkali metal cation (K^+, Rb^+, Cs^+, or one-charge Cu^+, Ag^+) has been proposed. To eliminate the toxicity of Pb, the idea of its substitution by other divalent cations outside of group IVA has been considered. However, it turned out that such compounds have less good optoelectric properties for use as solar cells (too wide band gap) [9]. In this direction the most promising substitutions in the structures of these compounds are two Pb^{2+} ions by one M^+ ion and one M^{3+} ion, or one M^{4+} ($2Pb^{2+} \rightarrow M^+ + M^{3+}$, $2Pb^{2+} \rightarrow M^{4+}$), maintaining the total number of valence electrons constant. As potential substitutes for Pb^{2+} compounds, halide double perovskites of the A_2B1B2X_6 type and vacancy-ordered double perovskites of the $A_2B\square X_6$ (where □ is a vacancy) type have been proposed [10-13].

Investigation of the reciprocal $K_2TeI_6 + Rb_2TeBr_6 \leftrightarrow K_2TeBr_6 + Rb_2TeI_6$ system is a necessary stage in the study of the system with double cation-cationic and anion-anionic substitution on the basis of A_2BX_6-type compounds.

The K(Rb)Br(I)–TeBr(I) systems feature $K_2(Rb_2)TeBr_6(I_6)$ compounds, which melt congruently [14,15]. The binary systems on the base of A_2TeX_6 (A = K, Rb, X = Br, I) compounds with cation-cationic or anion-anionic substitutions have

been investigated [16]. The K_2TeBr_6–Rb_2TeBr_6 and Rb_2TeBr_6–Rb_2TeI_6 systems are characterized by eutectic interaction, whereas the K_2TeI_6–Rb_2TeI_6 system belongs to the peritectic type. In the K_2TeBr_6–K_2TeI_6 system at high temperatures a eutectic process takes place, and at low temperatures an unlimited solid solution is formed.

2. Experimental details

The ternary compounds $K_2(Rb_2)TeBr_6(I_6)$ were synthesized by reacting stoichiometric amounts of high-purity elements, tellurium, bromine, iodine with purity not less than 99.8 wt.% and additionally purified by zone crystallization methods, binary KBr(I) and RbBr(I). The syntheses were performed by the direct two-temperature method at temperatures 50 K above T_{melt} of the ternary compounds (K_2TeBr_6 – 773 K, K_2TeI_6 – 733 K, Rb_2TeBr_6 – 1013 K, Rb_2TeI_6 – 843 K) in special two-section quartz ampoules. The heating was carried out at a rate of 40-60 K/h. Thermal treatment was carried out at the maximum temperature for 72 h (components and products of the interaction were in molten form, which led to completion of the chemical interaction with the formation of the necessary phases). Cooling was carried out at a rate of 20-30 K/h to an annealing temperature of 473 K (96 h annealing), followed by cooling of the ampoule in air. Alloys of the K_2TeBr_6–Rb_2TeI_6 system were synthesized from the ternary compounds along the whole concentration range with a step of 10 mol.%.

The obtained compounds and alloys were investigated by differential thermal analysis (DTA) (combined Chromel-Alumel thermocouples, automatic data recording on a computer, heating/cooling rates of 700 K/h, measurement accuracy ±5 K). X-ray powder diffraction was performed using a DRON 4-07 diffractometer (Cu K_α radiation, Ni-filter, scanning interval $10 \le 2\theta \le 60°$, scanning step 0.05°, exposure time 5 s). Crystal-chemical analysis and visualization were carried out using the program packages UnitCell (Holland-Redfern method) [17], PowderCell 2.3, Westa 3 [18], and Diamond 2. *Ab initio* quantum-mechanical calculations of the electronic structure were performed by the Quantum Espresso program (QE), which contains the core packages for the calculation of electronic-structure properties within the Density-Functional Theory (Plane-Wave basis set and pseudopotentials) [19,20].

3. Results and discussion

The crystal structure of perovskite with the general formula ABO_3 is cubic and is characterized by the presence of two types of position – cuboctahedral (coordination number CN = XII) and octahedral (CN = VI), occupied by atoms of the cations *A* and *B* (Fig. 1), respectively [21]. The BO_6 octahedra, which are connected by vertices, form an infinite three-dimensional framework, in the cavities of which are located *A*-cations surrounded by 12 oxygen atoms. The peculiarity of perovskites of the ABO_3 type is that when part of the *A* and *B* cations are replaced in the corresponding sublattice, the structure as a whole remains stable (the structure is tolerant). This allows not only isovalent substitutions, but also heterovalent ones, with a violation of the electroneutrality of the system, which leads to changes in the crystal structure, the formation of defects, accompanied by orthorhombic and rhombohedral deformations. Modification of the initial structural matrix of perovskite-type phases by iso- and heterovalent substitutions should lead to the appearance of a complex of important electrical-optical properties, which promotes their practical use [22,23].

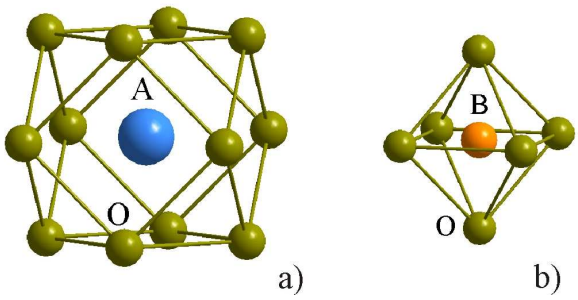

Fig. 1 Cuboctahedral (CN = XII) (a) and octahedral (CN = VI) (b) environment of *A* and *B* cations in the perovskite structure of the ABO_3 type.

An analysis of the physical-chemical interactions in the quasi-binary systems that form the reciprocal $K_2TeI_6 + Rb_2TeBr_6 \leftrightarrow K_2TeBr_6 + Rb_2TeI_6$ system, was performed on the basis of the electronic structures of the K(Rb), Te, and Br(I) atoms, thermodynamic stability and dimensional factors. According to the electronic configuration, the K(Rb) atoms in A_2TeX_6 ternary compounds act as cations, the Br(I) as anions, and Te as a central anion-forming atom.

The study of the crystallographic stability of materials in the perovskite structure within the idealized model of solid spheres is based on two empirical quantities (Goldschmidt's rule) – the tolerance factor (t) and the octahedral factor (μ). A statistical analysis of perovskite halides indicates that the formation of a perovskite structure requires $0.86 < t < 1.0$ and $\mu > 0.41$ [7]. Empirical values for the compounds $K_2(Rb_2)TeBr_6(I_6)$ were calculated according to the equations:

$$t = \frac{R_A + R_X}{\sqrt{2} \times (R_B + R_X)} \quad (1), \qquad \mu = \frac{R_B}{R_X} \quad (2).$$

For R_A, R_B, R_X we used ionic and crystalline radii according to Shannon and Pruitt (Table 1). The

calculations (Table 2) showed high stability of the individual ternary compounds and solid solutions based on them with the perovskite structure, especially the $Rb_2TeBr_6(I_6)$ compounds.

We considered the possibility of formation of unlimited solid solutions in the binary sections of the reciprocal $K_2TeI_6 + Rb_2TeBr_6 \leftrightarrow K_2TeBr_6 + Rb_2TeI_6$ system according to the quantitative criteria of Vozdvyzhensky [26] (Table 3).

$$n_s \leq 1.1 \div 1.2 \quad (3), \qquad 4n_t^2 + n_v^2 \leq 1.0 \quad (4),$$

where n_s – the entropy factor (ratio of entropies of melting S_A/S_B for $S_A>S_B$); n_t – the temperature factor equal to $1–T_A/T_B$ (for $T_A<T_B$) and $1–T_B/T_A$ (for $T_A>T_B$); n_v – volume or dimensional factor $[(d_A/d_B)^3+V_A/V_B–2]+b$ (d_A, d_B, V_A, V_B – size of the ions, volumes of unit cells, b – correction in valence differences).

The first criterion (n_s) characterizes the degree of homogeneity of the chemical bonds in the compounds, the second one ($4n_t^2+n_v^2$) the proximity of their physicochemical properties. Taking this into consideration the nature of the interaction between the ternary halides was studied for the possible formation of solid solutions.

Due to the polymorphous transformation of the K_2TeI_6 compound, the K_2TeBr_6–K_2TeI_6 system is characterized by eutectic interaction at high temperatures, which is confirmed by the deviation of the entropy factor from the condition $n_s > 1.1 \div 1.2$. At low temperatures an unlimited solid solution is formed (confirmed condition $4n_t^2+n_v^2 \leq 1$) (Table 3). The other systems based on the $K_2(Rb_2)TeBr_6(I_6)$ ternary compounds are characterized by the formation of boundary solid solutions (IV-V types of phase diagrams according to Roozeboom) (Fig. 2).

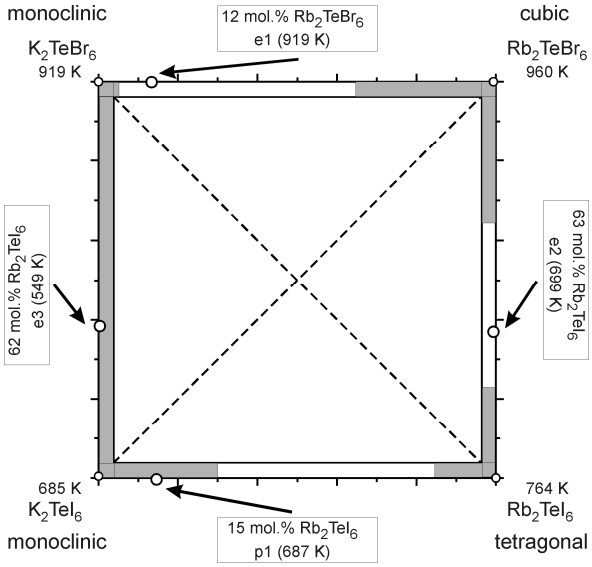

Fig. 2 Phase relations along the binary sections of the reciprocal $K_2TeI_6 + Rb_2TeBr_6 \leftrightarrow K_2TeBr_6 + Rb_2TeI_6$ system.

Table 1 Energy parameters of the elements that are part of the $K_2(Rb_2)TeBr_6(I_6)$ compounds.

Symbol	Electronic configuration	χ		r_{cov}, Å	r_{ion}, Å
		[24]	[24]	[24]	[25]
K	$[Ar]4s^1$	0.8	0.4	2.24 (octahedral)	(+1) 1.64 (CN XII)
Rb	$[Kr]5s^1$	0.8	0.4	2.56 (octahedral)	(+1) 1.72 (CN XII)
Te	$[Kr]5s^25p^4$	2.1	2.1	1.41 (tetrahedral)	(+4) 0.97 (CN VI)
Br	$[Ar]4s^24p^5$	2.8	3.0	1.22 (tetrahedral)	(–1) 1.96 (CN VI)
I	$[Kr]5s^25p^5$	2.5	2.8	1.40 (tetrahedral)	(–1) 2.20 (CN VI)

Table 2 Tolerance (t) and octahedral factors (μ) for $K_2(Rb_2)TeBr_6(I_6)$.

Compound	K_2TeBr_6	K_2TeI_6	Rb_2TeBr_6	Rb_2TeI_6
t	0.8688	0.8566	0.8881	0.8744
μ	0.4949	0.4409	0.4949	0.4409

Table 3 Quantitative criteria for the possibility of formation of solid solutions in the $K_2(Rb_2)TeBr_6(I_6)$ quasi-binary systems.

System	K_2TeBr_6	K_2TeI_6	Rb_2TeBr_6	Rb_2TeI_6	K_2TeBr_6	Rb_2TeBr_6	K_2TeI_6	Rb_2TeI_6
n_s	2.45		2.38		1.38		1.42	
n_t	0.25		0.204		4.38×10^{-2}		0.1034	
n_v	–0.4748		0.3064		–0.6942		–0.1265	
$4n_t^2+n_v^2$	0.4830		0.2606		0.4896		0.0588	

To study the direction of the exchange reaction (determination of the quasi-binary cross-section) in the reciprocal $K_2TeI_6 + Rb_2TeBr_6 \leftrightarrow K_2TeBr_6 + Rb_2TeI_6$ system the composition of the alloy at the intersection of the two possible cross-sections, was studied (Fig. 2). The diffraction pattern shows groups of reflections characteristic of monoclinic (K_2TeBr_6) and tetragonal (Rb_2TeI_6) phases. This fact indicates that the K_2TeBr_6–Rb_2TeI_6 section is quasi-binary and the direction of the exchange reaction is $K_2TeI_6 + Rb_2TeBr_6 \rightarrow K_2TeBr_6 + Rb_2TeI_6$.

Calculations of the quantitative criteria for the formation of solid solutions according to Vozdvyzhensky (equations 3,4) in the K_2TeBr_6–Rb_2TeI_6 system showed that the value of the entropy factor n_s=1.7272 ($n_s \geq 1.1 \div 1.2$) denies the possibility of formation of unlimited solid solutions, but the condition $4n_t^2+n_v^2 = 0.5816$ ($4n_t^2+n_v^2 \leq 1.0$) indicates the possibility of forming extended areas of solid solutions based on the $K_2(Rb_2)TeBr_6(I_6)$ ternary compounds.

The K_2TeBr_6–Rb_2TeI_6 system (Fig. 3) is the quasi-binary section of the reciprocal $K_2TeI_6 + Rb_2TeBr_6 \leftrightarrow K_2TeBr_6 + Rb_2TeI_6$ system and is characterized by eutectic interaction (V type of phase diagrams according to Roozeboom) with the formation of boundary solid solutions α on the basis of K_2TeBr_6 and β on the basis of Rb_2TeI_6. The lines of primary crystallization cross at the eutectic point ($L \leftrightarrow \alpha+\beta$ invariant process) with the coordinates 58 mol.% Rb_2TeI_6, 715 K. The length of the solid solutions at the temperature of the invariant eutectic process are up to 35 mol.% for the α-phase and up to 25 mol.% for the β-phase. At the temperature of the homogenizing annealing, 473 K, the solid solutions extend up to 25 mol.% for the α-phase and up to 15 mol.% for the β-phase. The formation of boundary solid solutions is due to the crystallization of ternary compounds in different crystal structures: K_2TeBr_6 is monoclinic, whereas Rb_2TeI_6 is tetragonal (Table 4). On increasing the radius ratio from $r_{(Rb)}/r_{(I)}$ = 0.72 to $r_{(K)}/r_{(Br)}$ = 0.84 there is a transition from tetragonal to monoclinic structure (Fig. 4).

Crystal-chemical analyses showed that the $K_2(Rb_2)TeBr_6(I_6)$ compounds crystallize in the structure type K_2PtCl_6 [27-30]. The coordination octahedra [TeX_6] are formed by six halogen atoms (X) surrounding the Te atom and located at the vertices of regular tetragonal bipyramids. The coordination octahedra [TeX_6] are located at the vertices and the center of a large cube; the K^+, Rb^+ ions/atoms are placed between them (Fig. 4).

To establish the type of chemical bond in the $K_2TeBr_6(I_6)$ and $Rb_2TeBr_6(I_6)$ ternary compounds the interatomic distances were compared with the sum of the covalent and ionic radii of the atoms (Fig. 5, Table 5).

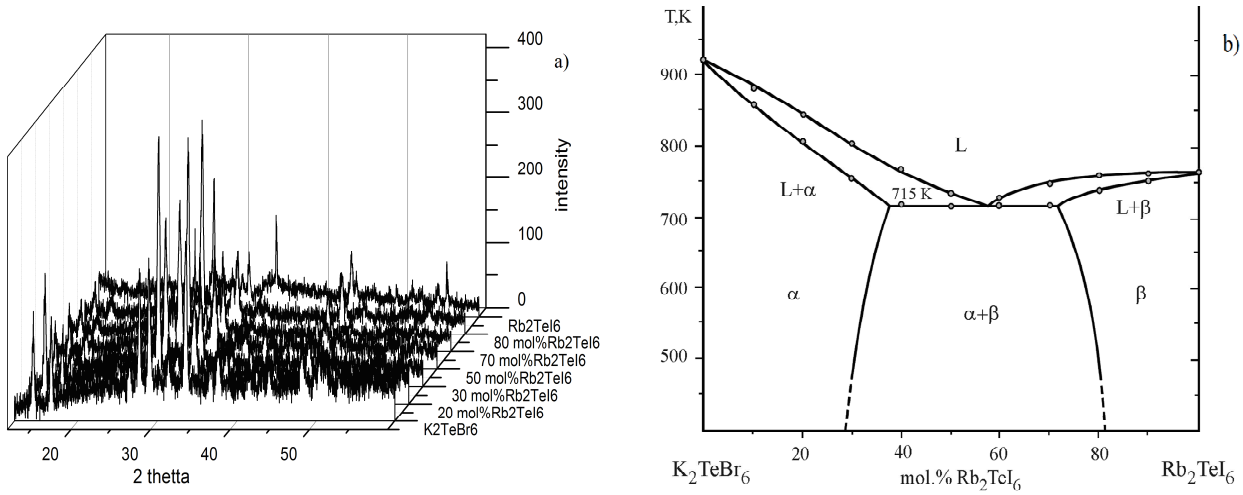

Fig. 3 X-ray powder diffraction patterns (a) and phase diagram (b) of the K_2TeBr_6–Rb_2TeI_6 quasi-binary system.

Table 4 Crystal-chemical parameters of the $K_2(Rb_2)TeBr_6(I_6)$ compounds.

Compound	Crystal symmetry	Space group	Lattice parameters
K_2TeBr_6 [27]	monoclinic	$P12_1/c1$	a = 7.4908, b = 7.5492, c = 13.0272 Å, β = 124.79, V = 604.98 Å^3
K_2TeI_6 [28]	monoclinic	$P12_1/c1$	a = 7.9850, b = 8.1710, c = 13.9281 Å, β = 124.50, V = 748.93 Å^3
Rb_2TeBr_6 [29]	cubic	Fm-3m	a = 10.7730, V = 1250.29 Å^3
Rb_2TeI_6 [30]	tetragonal	$P4/mnc$	a = 8.1360, c = 11.8100 Å, V = 781.76 Å^3

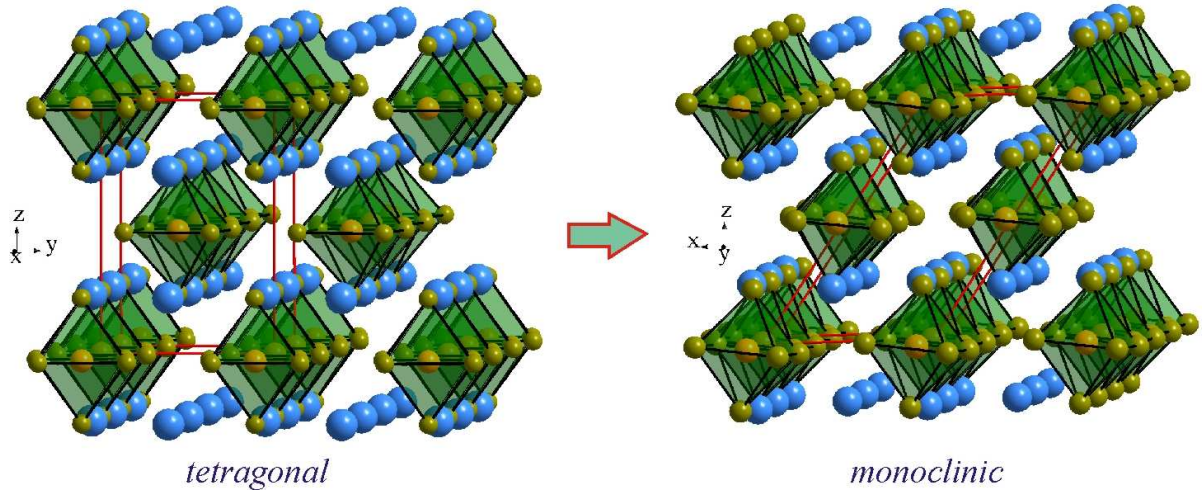

Fig. 4 Transition from the tetragonal structure of Rb_2TeI_6 to the monoclinic structure of K_2TeBr_6.

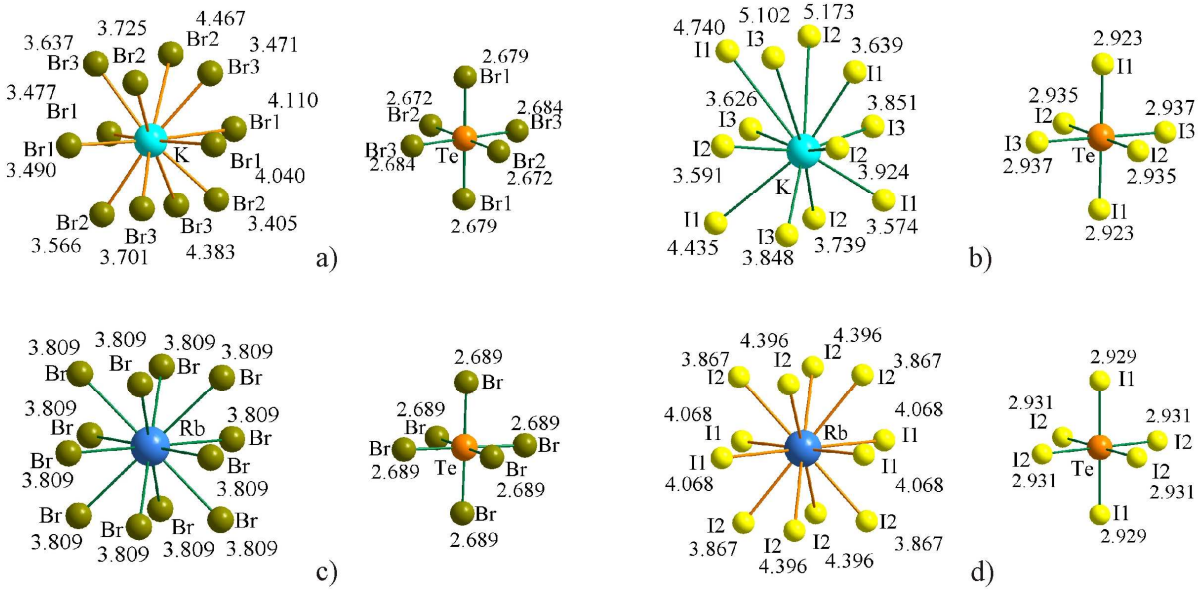

Fig. 5 Coordination environment and interatomic distances in the structures of K_2TeBr_6 (a), K_2TeI_6 (b), Rb_2TeBr_6 (c), and Rb_2TeI_6 (d).

Table 5 Interatomic distances (Å) in the crystal structures of $K_2(Rb_2)TeBr_6(I_6)$.

Bonds	$K_2TeBr_6(I_6)$ (exp)	$Rb_2TeBr_6(I_6)$ (exp)	Σ cov. (calc)	Σ ion. (calc)	S_I [a]
K – Br	3.405-4.467	–	3.46	3.60	77
K – I	3.574-5.173	–	3.64	3.84	73
Rb – Br	–	3.809	3.78	3.62	77
Rb – I	–	3.867-4.339	3.96	3.92	73
Te – Br	2.672-2.684	2.689	2.63	2.93	32
Te – I	2.923-2.937	2.929-2.931	2.81	3.17	26
Br – Br	3.770-3.8043	3.803	2.44	3.92	0
I – I	4.131-4.1733	4.144-4.145	2.80	4.40	0

[a] S_i is the degree of ionicity of the bond in the crystals.

The analysis of the interatomic distances in the A_2TeX_6 compounds showed that the experimental distances *A*–*X* are slightly longer than the calculated sum of the ionic radii of the corresponding atoms. This indicates that these bonds are clearly ionic in nature. When K is replaced by Rb, an increase in the interatomic distances *A*–*X* is observed, which indicates an increase in the degree of ionicity of the chemical bond. The values of the Te–*X* interatomic distances are slightly larger than the sum of the covalent and smaller than the sum of the ionic radii of the atoms, which indicates covalent nature of the corresponding bonds. With Br→I substitution, due to the increase of the covalent radii, an increase of the interatomic distances Te–*X* and, at the same time, a decrease of the degree of ionicity of the chemical bonds, is observed. The values of the interatomic distances Te–*X* change insignificantly when K is replaced by Rb, which underlines the stability of the complex ion $[TeX_6]^{2-}$. The analysis of the results indicates that the chemical bonding in ternary A_2TeX_6-type halide compounds has a mixed chemical bond type – iono-covalent with predominance of the ionic component. In fact, compounds of this type can be considered as ionic compounds, where the role of the cation is played by the element *A*, and the role of the anion by the stable complex ion $[TeX_6]^{2-}$. In the A_2TeX_6-type complex compounds an increase in the ionicity of the *A*–*X* bond caused by the replacement of K by Rb in the outer coordination sphere leads to an increase in the degree of covalence of the bonding in the inner sphere of the complex ion $[TeX_6]^{2-}$. Since the change in the electronegativity of the alkali metal atoms occurs symbatically with the change of their ionic radii, the obtained results are in good agreement with the compensatory dependence – the smaller the size of the outer spherical cation, the larger the overall size of the complex anion.

We considered the structure of the octahedral $[TeX_6]^{2-}$ complex ions within the ligand field theory (LFT) and the molecular orbital (MO) method, in which only σ-bonds are present (Fig. 6). The overlap of the orbitals of the central atom and the six ligands contributes to a series of molecular orbitals.

During the formation of the Te^{4+} ion, the $5p^4$-electrons are separated. Paired $5s^2$-electrons do not come off, which is due to the 4*d*-level shielding. In an isolated Te^{4+} ion, the 4*d* orbitals are completely filled with ten paired electrons and do not participate in the formation of bonds. The five 5*d* orbitals of the external energy level are closer to the ligand ions than the 4*d* orbitals of the penultimate level, which leads to a denser overlap of d_{z^2} and $d_{x^2-y^2}$ orbitals with the *p* orbitals of the halogen ions with the formation of two molecular bonding e_g orbitals. The d_{xz}, d_{xy}, and d_{yz} orbitals do not directly participate in the formation of bonds with halogens and form t_{2g} nonbonding MO. Free 5*p* and 5*s* orbitals filled with two paired electrons, in turn, form four bonding (one a_{1g} and three t_{1u}) molecular orbitals. 12 of the 14 valence electrons (2 electrons of the Te^{4+} ion and 12 electrons of the ligands – halogen ions X^-) are located in the a_{1g}, t_{1u}, and e_g bonding molecular orbitals. The other two electrons are located in t_{2g} nonbonding orbitals. The presence of unpaired electrons in t_{2g} is confirmed by the fact that in the complexes there is a distortion of the octahedral configuration (the configuration of a tetragonal bipyramid – distorted octahedron – is more stable) if the complexing agent contains in its *d* orbitals nonbound electrons, asymmetrically with respect to the others (resulting in deformation of the structure). For the same ligand X^-, in the direction Rb^+ to K^+, a decrease in the symmetry of the polyatomic complex A_2TeX_6 from tetragonal (cubic) to monoclinic is observed.

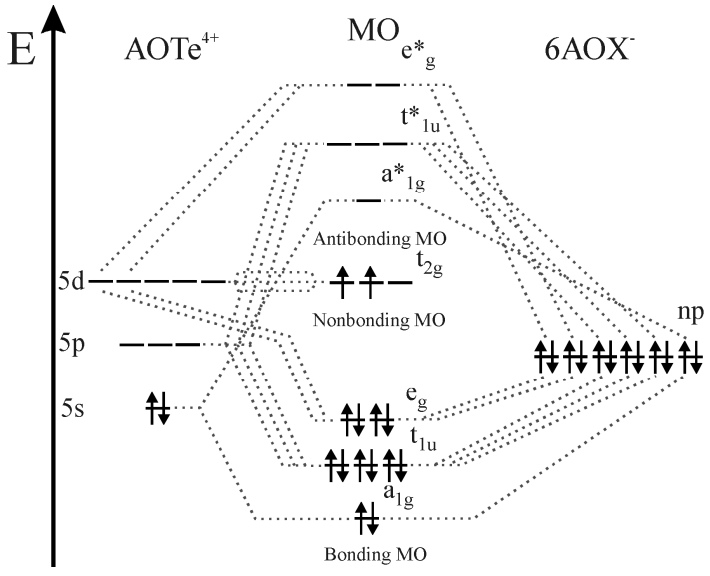

Fig. 6 Distribution of the electrons in the molecular orbitals of the complex ion $[TeX_6]^{2-}$ (*X* = halogen).

Ab initio quantum-mechanical calculations of the electronic structure of the $K_2(Rb_2)TeBr_6(I_6)$ compounds were performed by the density functional theory (DFT) method (Quantum Espresso package). The structure geometry was optimized using the self-consistent field method (SCF) based on the Bruden–Fletcher–Goldfarb–Shanno (BFGS) algorithm. The band structure calculations for the $K_2(Rb_2)TeBr_6(I_6)$ compounds were performed along the lines that connect the high-symmetry points of the first Brillouin zone (BZ) (Fig. 7). Based on the theoretical band-structure calculations, the total density of states (DOS) of the energy distribution of the electronic states within the valence-band and conduction area were determined (Fig. 8). Results of the DFT calculations (semiconductor type, unit-cell energy, energy per atom, Fermi energy, band gap) are presented in Table 6.

In order to characterize the origin of the energy levels, the total and different partial densities of states were calculated. As one can see from Fig. 8, the top of the valence band is formed by 4*p* electrons of bromine (or 5*p* of iodine), while the bottom of the conduction band is formed by 5*d* states of Te and 5*s* states of Br (or 6*s* states of I). The optical band gap can be created by Br(I) $4p(5p) \rightarrow$ Br(I) $5s(6s)$ or by Te 5*d* electrons. The potassium 4*s* states are located at -10.8 eV, 3*p* at -13.8 and -12.3 eV, rubidium 5*s* at -10.6 eV, 4*p* at -26.4 eV. The levels of the tellurium atom are -10.8 eV (4*s*), -3.9÷-4.5 eV (4*p*) and -12.4÷-13.6 eV (3*d*). The levels of the halogen atoms are Br 4*s* (-15.0 and -13.8 eV), Br 4*p* (series of peaks -2.9÷-1.9 eV), I 5*s* (-15.6, -12.1 and -10.8 eV), I 5*p* (series of peaks -2.9÷-1.5 eV).

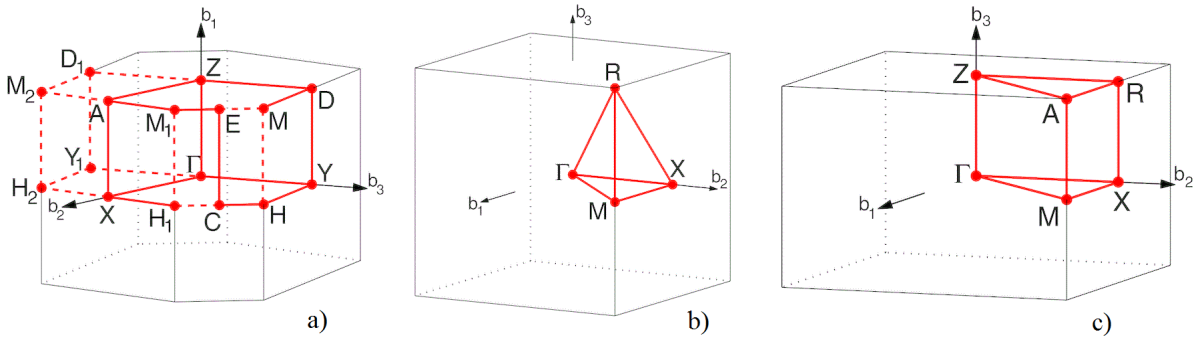

Fig. 7 First Brillouin zone of the primitive monoclinic (a), primitive tetragonal (b), and primitive cubic (c) lattices [31].

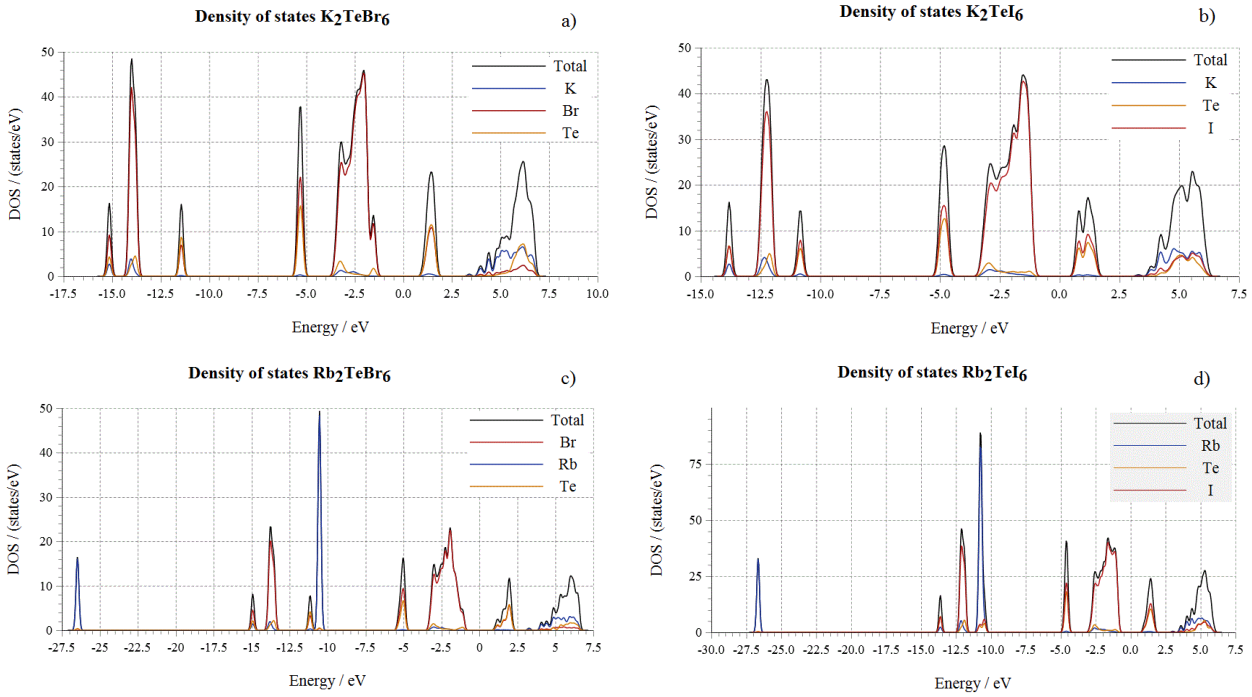

Fig. 8 Total and partial DOS of K_2TeBr_6 (a), K_2TeI_6 (b), Rb_2TeBr_6 (c), and Rb_2TeI_6 (d).

Table 6 Characteristic parameters of the electronic structures of $K_2(Rb_2)TeBr6(I_6)$.

Compound	Semiconductor type	E_{uc}, eV	E/atom, eV	E_{Fermi}, eV	VB_{max}, eV	CB_{min}, eV	E_g, eV
K_2TeBr_6	indirect	-26.28	-2.92	2.61	-1.42	0.91	2.39
K_2TeI_6	indirect	-22.97	-2.55	2.81	-1.06	0.68	1.74
Rb_2TeBr_6	indirect	-21.72	-2.41	2.93	-1.02	1.05	2.07
Rb_2TeI_6	indirect	-40.14	-4.46	2.91	-0.81	0.91	1.72

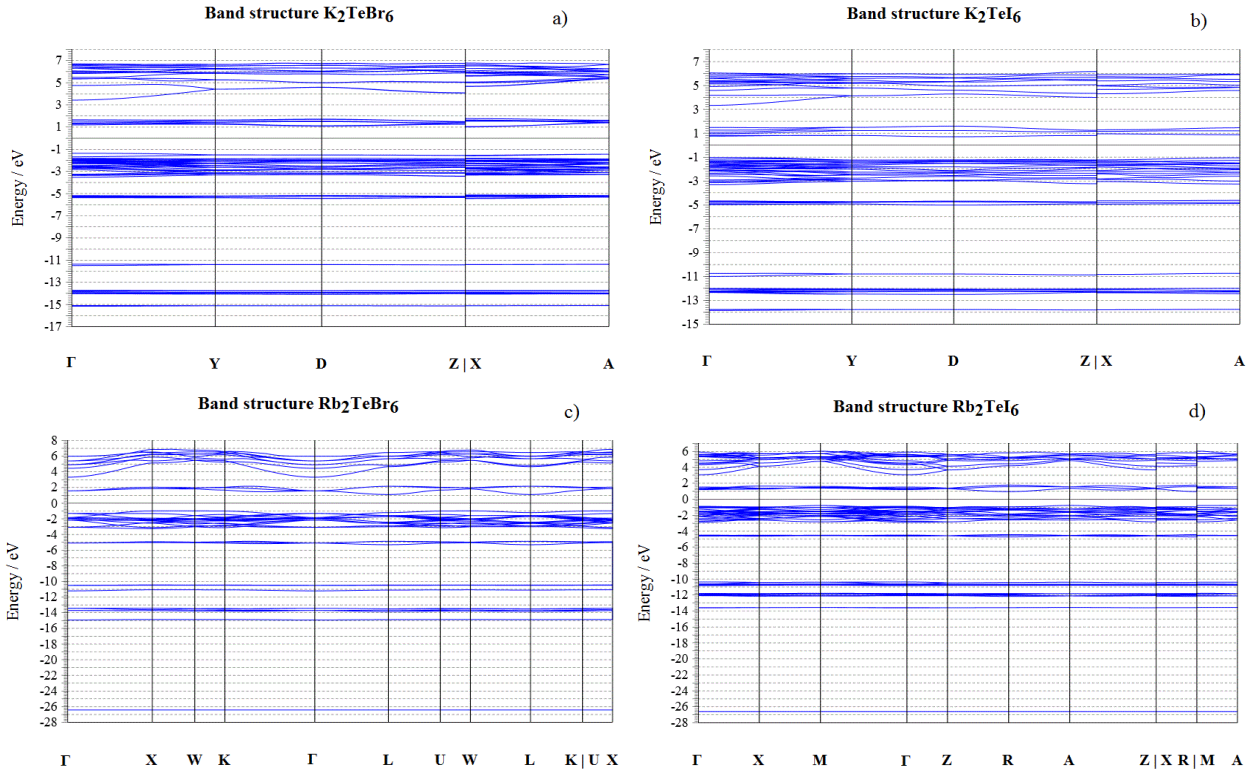

Fig. 9 Band structures of K_2TeBr_6 (a), K_2TeI_6 (b), Rb_2TeBr_6 (c), and Rb_2TeI_6 (d).

Fig. 9 shows that the calculated band gaps are equal to E_g = 2.39 eV (K_2TeBr_6), E_g = 1.74 eV (K_2TeI_6), E_g = 2.07 eV (Rb_2TeBr_6), and E_g = 1.72 eV (Rb_2TeI_6). At the substitutions K→Rb and Br→I the width of the forbidden zone naturally decreases, which is explained by an increase of the metal component of the chemical bond. The values of the Fermi energy (E_{Fermi}) for the Rb-containing compounds are also higher than those of the K-containing compounds. The valence band maximum (VB_{max}) and conduction band minimum (CB_{min}) are located in different points of the BZ. This indicates that the calculated band gaps are of indirect type for all the $K_2(Rb_2)TeBr_6(I_6)$ compounds.

4. Conclusions

The calculation of empirical quantities (tolerance factor t and octahedral factor μ according to Goldschmidt's rule) indicate high stability of the individual $K_2(Rb_2)TeBr_6(I_6)$ compounds. The possibility of extended solid solutions based on the perovskite structures in the reciprocal system $K_2TeI_6 + Rb_2TeBr_6 \leftrightarrow K_2TeBr_6 + Rb_2TeI_6$ was confirmed using the quantitative criteria of Vozdvyzhensky. Differential thermal analysis and X-ray diffraction were used to construct for the first time the phase diagram of the K_2TeBr_6–Rb_2TeI_6 system. The character of the monovariant processes, the temperature and coordinates of the invariant eutectic process (58 mol.% Rb_2TeI_6, 715 K) in the quasi-binary system were determined. The existence of solid solutions of the K_2TeBr_6 and Rb_2TeI_6 ternary compounds was established. The crystal structures of the ternary compounds, changes in the type of chemical bond by cation-cationic (K→Rb) and anion-anionic (Br→I) substitutions were analyzed. *Ab initio* quantum-mechanical calculations of the electronic structure by the DFT method showed that the $K_2(Rb_2)TeBr_6(I_6)$ compounds belong to the class of indirect-type semiconductors with band gaps of E_g = 2.39 eV (K_2TeBr_6), E_g = 1.74 eV (K_2TeI_6),

E_g = 2.07 eV (Rb_2TeBr_6), and E_g = 1.72 eV (Rb_2TeI_6). The solid solutions that form in the reciprocal $K_2TeI_6 + Rb_2TeBr_6 \leftrightarrow K_2TeBr_6 + Rb_2TeI_6$ system, may serve as new semiconductor materials with a complex of appropriate physical and optical properties.

References

[1] N.J. Jeon, J.H. Noh, W.S. Yang, Y.C. Kim, S. Ryu, J. Seo, S.I. Seok, *Nature* 517(7535) (2015) 476-480. https://doi.org/10.1038/nature14133

[2] D.P. McMeekin, G. Sadoughi, W. Rehman, G.E. Eperon, M. Saliba, M.T. Hörantner, A. Haghighirad, N. Sakai, L. Korte, B. Rech, M.B. Johnston, L.M. Herz, H.J Snaith, *Science* 351(6269) (2016) 151-155. https://doi.org/10.1126/science.aad5845

[3] D. Bi, B. Xu, P. Gao, L. Sun, M. Grätzel, A. Hagfeldt, *Nano Energy* 23 (2016) 138-144. https://doi.org/10.1038/srep42564

[4] G. Niu, X. Guo, L. Wang, *J. Mater. Chem. A* 3(17) (2015) 8970-8980. https://doi.org/10.1039/C4TA04994B

[5] M.R. Filip, F. Giustino, *J. Phys. Chem. C* 120(1) (2016) 166-173. https://doi.org/10.1021/acs.jpcc.5b11845

[6] S. Körbel, M.A. Marques, S.Botti, *J. Mater. Chem. C* 4(15) (2016) 3157-3167. https://doi.org/10.1039/C5TC04172D

[7] T.J. Jacobsson, M. Pazoki, A. Hagfeldt, T. Edvinsson, *J. Phys. Chem. C* 119(46) *(*2015) 25673-25683. https://doi.org/10.1021/acs.jpcc.5b06436

[8] E. Mosconi, A. Amat, Md. K. Nazeeruddin, M. Gratzel, F. De Angelis, *J. Phys. Chem. C* 117(27) (2013) 13902-13913. https://doi.org/10.1021/jp4048659

[9] S.F. Hoefler, G. Trimmel, T. Rath, *Monatsh. Chem*. 148 (2017) 795-826. https://doi.org/10.1007/s00706-017-1933-9

[10] A.E. Maughan, A.M. Ganose, M.M. Bordelon, E.M. Miller, D.O. Scanlon, J.R. Neilson, *J. Am. Chem. Soc*. 138 (2016) 8453-8464. https://doi.org/10.1021/jacs.6b03207

[11] G. Volonakis, A.A. Haghighirad, R.L. Milot, W.H. Sio, M.R. Filip, B. Wenger, M.B. Johnston, L.M. Herz, H.J. Snaith, F. Giustino, *J. Phys. Chem. Lett*. 8 (2017) 772-778. https://doi.org/10.1021/acs.jpclett.6b02682

[12] Xin-Gang Zhao, Ji-Hui Yang, Fu Yuhao, Yang Dongwen, Xu Qiaoling, Yu Liping, Wei Su-Huai, Lijun Zhang, *J. Am. Chem. Soc*. 139 (2017) 2630-2638. https://doi.org/10.1021/jacs.6b09645

[13] M.R. Linaburg, E.T. McClure, J.D. Majher, P.M. Woodward, *Chem. Mater*. 29(8) (2017) 3507-3514. https://doi.org/10.1021/acs.chemmater.6b05372

[14] E. Peresh, V. Sidey, O. Zubaka, *Neorg. Mater*. 41(3) (2002) 357-362 (in Russian).

[15]. E. Peresh, O. Zubaka, V. Sidey, I. Barchii, S. Kun, A. Kun, *Neorg. Mater*. 38(8) (2002) 1020-1024 (in Russian).

[16] I. Barchiy, *Nauk. Visn. Uzhhorod. Univ., Ser. Khim*.10 (2003) 3-8 (in Ukrainian).

[17] T.J.B. Holland, S.A.T. Redfern, *Mineral. Mag.* 61 (1997) 65-77. https://doi.org/10.1180/minmag.1997.061.404.07

[18] W.J. Kraus, *J. Appl. Crystallogr*. 29(3) (1996) 301-303. https://doi.org/10.1107/S0021889895014920

[19] P. Giannozzi, O. Andreussi, T. Brumme, *et al.*, *J. Phys.: Condens. Matter* 29(46) (2017) 465901. https://doi.org/10.1088/1361-648X/aa8f79

[20] A. Dal Corso, In: C. Pisani (Ed.), *Quantum-Mechanical Ab-initio Calculation of the Properties of Crystalline Materials*, LNC, Vol. 67, Springer, Berlin, Heidelberg, 1996, pp. 155-178. https://doi.org/10.1007/978-3-642-61478-1_10

[21] R. Liu, Y. Xuan, Y.Q.Jia, *Mater. Chem. Phys*. 57 (1998) 81-85.

[22] N. Hara, F. Munakata, Y. Iwasaki, *J. Electrochem. Soc*. 145(1) (1998) 99-106.

[23] C.A. Randall, A.S. Bhalla, T.R. Shrout, *J. Mater. Res*. 5 (1990), 829-834. https://doi.org/10.1557/JMR.1990.0829

[24] S. Batzanov, *Experimental Fundamentals of Structural Chemistry*, Moscow, 1986, 240 p. (in Russian).

[25] R.D. Shannon, *Acta Crystallogr. A* 32 (1976) 751-767.

[26] I. Barchiy, E. Peresh, V. Rizak, V. Hudoliy, *Heterogeneous Systems*. Uzhhorod, 2003, 212 p. (in Ukrainian).

[27] S.C. Abrahams, J. Ihringer, P. Marsh, *Acta Crystallogr. B* 45 (1989) 26-34.

[28] S. Syoyama, K. Osaki, S.Kusanagi, *Inorg. Nucl. Chem. Lett*. 8 (1972) 181-184.

[29] W. Abriel, J. Ihringer, *J. Solid State Chem*. 52 (1984) 274-280.

[30] W. Abriel, *Mater. Res. Bull*. 17 (1982) 1341-1346.

[31] W. Setyawan, S. Curtarolo, *Comput. Mater. Sci*. 49 (2010) 299-312 https://doi.org/10.1016/j.commatsci.2010.05.010